Nano Today (2012) 7, 158—167

Available online at www.sciencedirect.com

SciVerse ScienceDirect

journal homepage: www.elsevier.com/locate/nanotoday

RAPID COMMUNICATION

Guided delivery of polymer therapeutics using plasmonic photothermal therapy

Adam J. Gormley[a,b,1], Nate Larson[b,c,1], Shraddha Sadekar[b,c], Ryan Robinson[a,b], Abhijit Ray[b,c], Hamidreza Ghandehari[a,b,c,*]

[a] Department of Bioengineering, University of Utah, Salt Lake City, UT 84112, USA
[b] Center for Nanomedicine, Nano Institute of Utah, University of Utah, Salt Lake City, UT 84112, USA
[c] Department of Pharmaceutics and Pharmaceutical Chemistry, University of Utah, Salt Lake City, UT 84112, USA

Received 2 February 2012; received in revised form 13 April 2012; accepted 21 April 2012
Available online 24 May 2012

KEYWORDS
Polymer therapeutics;
Gold nanorod;
Hyperthermia;
Prostate cancer;
GRP78;
Photothermal therapy

Summary In most drug delivery systems the clinician does not have control over the location of drug delivery after the therapeutic has been administered. As the location of the tumor mass is often known in many patients, a therapy system which enables the clinician to play an active role in nanomedicine localization would provide an advantage. Here, we show a new approach wherein a laser can be used to tag tumor tissue and enhance the delivery of targeted polymer therapeutics. Plasmonic gold nanorods are delivered to the cancerous tissue and heated by a laser to promote a targetable, hyperthermic response. Concurrent administration of a heat shock targeted polymer therapeutic thereby enhances site specific delivery.

Introduction

Incorporation of anticancer agents within nanocarriers represents an effective way of delivering hydrophobic drugs in the blood as well as altering their organ distribution in the body [1]. These nanomedicines have been designed to target sites of disease and enhance delivery to solid tumors. Despite substantial progress, clinical translation has been slow due to limited accumulation in the target site [2].

The delivery of targeted nanomedicines to solid tumors utilizes a two-pronged approach [1]. First, their nanoscale size (~5—500 nm) is leveraged to reduce the accumulation in healthy organs while maximizing extravasation into the tumor mass. While the junctions between vascular endothelial cells in healthy tissues are too small (~2—6 nm) to allow permeation, larger gaps (up to 1.2 μm), which are present in the tumor's poorly developed and leaky vasculature, allow them to partition out of the blood and into the tumor mass [3]. Described as the enhanced permeability and retention (EPR) effect [4], this passive targeting approach has been applied ubiquitously in the delivery of nanomedicines [5]. Second, once in the tumor interstitial space, contact with receptors expressed on the cancer cell surface immobilizes them and triggers their internalization via endocytosis followed by drug release [6]. This binding and uptake can be

* Corresponding author at: 5215 SMBB, 36 S. Wasatch Dr., Salt Lake City, UT 84112-5001, USA. Tel.: +1 801 587 1566.
E-mail address: hamid.ghandehari@pharm.utah.edu (H. Ghandehari).
[1] These authors contributed equally to this work.

1748-0132/$ — see front matter © 2012 Elsevier Ltd. All rights reserved.
http://dx.doi.org/10.1016/j.nantod.2012.04.002

further increased through active targeting by conjugating receptor specific ligands to the nanocarriers [7].

Polymer-based nanomedicines have the advantage of solubilizing hydrophobic drugs and exhibiting stealth-like characteristics thereby evading immune recognition [8]. In such systems drugs can be covalently linked to the polymer backbone and specifically released by enzymatic degradation or hydrolysis [9]. These polymer-drug conjugates are typically 5—15 nm in hydrodynamic diameter and can therefore be cleared by urinary excretion [10]. This is advantageous due to rising safety concerns of nanomedicines which are not eliminated from the body [11—14]. The small size however comes with a cost as rapid renal elimination reduces the availability of the conjugates to accumulate in tumors by the EPR effect [15]. With these advantages and limitations in mind, there is therefore a need to develop a strategy which maximizes the delivery of polymer therapeutics within the window of opportunity before renal clearance.

This need is particularly apparent considering conjugates, which aim to maximize tumor delivery, have to date demonstrated only moderate clinical benefit. For example, early generation polymer-drug conjugates such as *N*-(2-hydroxypropyl)methacrylamide (HPMA) copolymer-doxorubicin and poly(ethylene glycol) (PEG)-camptothecin have not obtained the same success in the clinic as other nanomedicines such as Doxil® (liposome-doxorubicin) and Abraxane® (albumin-paclitaxel) [8]. While much of this may be related to other variables such as drug release kinetics, the lack of sufficient delivery to the tumor ($\ll$15% of the injected dose) represents the primary barrier to success. Recent efforts to improve this delivery such as using high molecular weight biodegradable polymers which exhibit prolonged blood circulation as well as using polymers with different architectures (i.e. dendrimers and branched polymers) have achieved some success. However, greater control over both passive and active targeting strategies is desirable [16].

One method which has been described as a temporary means of enhancing the delivery of macromolecules such as albumin, liposomes and other nanomedicines is by inducing tumor hyperthermia [17—22]. Under conditions of elevated temperatures and increased blood perfusion, it has been found that the tumor microvascular permeability and therefore EPR effect is significantly increased [23]. This is believed to be a result of cytoskeletal disaggregation in endothelial cells leading to further expansion of the fenestrae that already surround them [24—27]. Unfortunately, current techniques for inducing tumor hyperthermia such as radiofrequency ablation or hyperthermic intraperitoneal perfusion are restrictive in their capacity to selectively deliver heat towards cancerous tissue [28].

More recently several laboratories have initiated hyperthermia by taking advantage of unique nanoscale events that occur when light is absorbed by plasmonic gold nanostructures. In brief, when light with a wavelength that matches the tunable surface plasmon resonance (SPR) of gold nanostructures interacts with these particles, coherent oscillations of electrons in the conduction band allow the light to be absorbed and photothermal conversion to occur [29]. When such particles are delivered to cancerous tissue by EPR, this phenomenon can be used as a tool to selectively induce hyperthermia [30]. Such plasmonic photothermal therapy has been used to achieve tumor selective temperatures varying from 50 °C to over 70 °C, well above the threshold required for vascular damage [31—35]. Previously, it has been shown in our lab as well as others that this heat delivery technique at reduced temperatures (42—45 °C) can be applied to selectively increase the perfusion and permeability of the tumor vasculature and hence the delivery of nanomedicines during laser radiation [36—40]. In this way, the delivery of nanoworms, liposomes and micelles have shown to be recruited to the treatment site and sensitized for targeting and drug release [38—40].

In this work, we aim to remotely modify the tumor microenvironment with laser mediated plasmonic photothermal therapy to increase both passive and active polymeric drug targeting. We use this technique immediately following injection of HPMA copolymers to augment EPR at the treatment site and drive their delivery into the tumor interstitial space while the copolymer is at its peak concentration in the blood (Fig. 1). Once at the tumor site, we take advantage of the natural response of tissue to heat shock by conjugation of a targeting ligand which binds to heat shock proteins (HSPs). This is because the expression of HSPs is significantly increased following exposure to heat shock [26]. In this way, the targetability of these cancer cells can be elevated so that the copolymer is retained in the tumor and taken up by cells to a higher extent.

We therefore introduce a technique wherein a laser can be used to direct the localization and retention of polymer therapeutics in solid tumors. With this technique, we believe that polymer-drug conjugates can be administered to patients by clinicians and efficiently guided towards the location of disease to maximize treatment efficacy, while minimizing toxicity.

Material and methods

Synthesis and characterization of PEGylated gold nanorods

Gold nanorods were synthesized using the seed-mediated growth method [41]. Optimization of silver nitrate content and seed amount yielded gold nanorods with an aspect ratio such that the SPR peak was between 800 and 810 nm. The gold nanorods were then centrifuged and washed three times with deionized water to remove excess hexadecyltrimethylammonium bromide (CTAB). PEGylation was done by addition of methoxy-PEG-thiol (5 kD, Creative PEGWorks, Winston Salem, NC) to the gold nanorod suspension. The suspension was then thoroughly dialyzed against deionized water and sterile filtered. In the final step, the gold nanorods were centrifuged, washed three times with DI water to remove unreacted PEG and concentrated. The final product was stored at 4 °C for a maximum of two months before use. The size and shape of the gold nanorods were determined by transmission electron microscopy (TEM) and the light absorption profile was measured by UV spectrometry. Zeta potential was measured in DI water by measuring electrophoretic mobility using laser Doppler velocimetry (Zetasizer Nano ZS, Malvern Instruments Ltd, Worcestershire, UK).

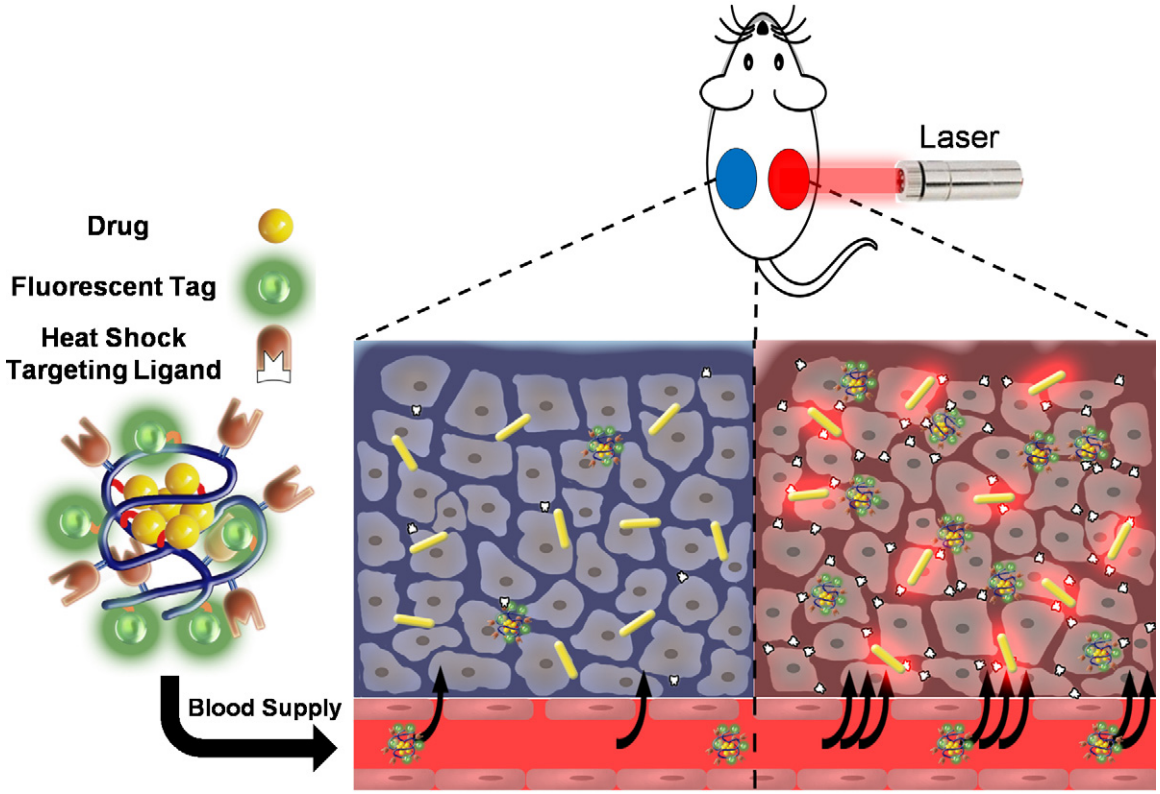

Figure 1 *Schematic of laser guided approach*. Following delivery of gold nanorods to tumors, a laser is applied to the right tumor to heat the gold nanorods and induce a heat shock response. This effectively increases the pore size in the tumor vasculature as well as the cell surface expression of heat shock proteins (HSPs), resulting in increased tumor accumulation and retention.

Synthesis and characterization of HPMA copolymer-drug conjugates

The comonomers were synthesized as described previously [42,43]. Precursor copolymer conjugates containing reactive carboxyl groups (thiazolidine-2-thione) were prepared by free radical copolymerization in methanol using azobisisobutryonitrile (AIBN) as initiator. For the conjugates containing drug, aminohexylgeldanamycin (AHGDM) was conjugated to the *N*-methacryloylglycylphenylalanylleucylglycine (MA-GFLG-OH) lysosomally cleavable linker prior to copolymerization. Finally, copolymerization with the monomer *N*-methacryloyl-tyrosinamide (MA-Tyr-$CONH_2$) allows for radiolabeling of the conjugates or 5-[3-(methacryloylaminopropyl)thioureidyl] fluorescein (APMA-FITC) for fluorescent tracking of cellular uptake in cells. Heat shock targeted conjugates were obtained by aminolysis of precursor copolymers with the GRP78 targeting peptide (WIFPWIQL), synthesized by solid phase. Untargeted conjugates were obtained by hydrolysis of precursor copolymers in the presence of aqueous sodium hydroxide. Copolymer conjugates were purified by dialysis against deionized water, lyophilized, and stored at −20 °C. Weight average molecular weight (M_w), number average molecular weight (M_n), and polydispersity (M_w/M_n) were estimated by size exclusion chromatography (SEC) using HPMA homopolymer fractions of known molecular weight. The amount of the anticancer agent AHGDM present was quantified by UV spectrometry, and the amount of the GRP78 targeting peptide was quantified by amino acid analysis (HPLC method). ^{125}Iodine was conjugated to tyrosine residues to obtain radiolabeled copolymers using the Iodogen method with slight modification [44]. Each copolymer (2 mg) and 0.5 mCi Na−^{125}I were dissolved in 0.5 M NaH_2PO_4 pH 7.0 and incubated at room temperature in Iodogen tubes for 10 min. Free radiolabel was removed by dialysis against saline and verified by SEC.

In vitro cell surface GRP78 expression

Cell surface GRP78 expression was evaluated as a function of time by flow cytometry. Human prostate cancer DU145 cells were subjected to heat shock (43 °C/30 min incubation) or control (37 °C, continuous incubation). At each time point, cells were removed and incubated with an anti-GRP78 rabbit polyclonal antibody (Enzo Life Sciences, Farmingdale, NY) followed by incubation with a goat anti-rabbit phycoerythrin (PE) conjugated secondary antibody (Santa Cruz Biotechnology, Santa Cruz, CA). Cells were then fixed in 1% formaldehyde in phosphate buffered saline (PBS) and analyzed by flow cytometry. Incubation with secondary antibody alone served as an additional control for non-specific binding.

Cellular uptake of FITC-labeled conjugates

Cellular uptake was evaluated qualitatively by confocal microscopy. DU145 cells were exposed to heat shock

(43 °C/30 min incubation) or control (37 °C, continuous incubation). Eight hours post-heat shock, cells were incubated with 0.5 mg/mL of heat shock targeted or untargeted conjugates for four hours. Cells were then washed, plasma membrane stained with TRITC-lectin (10 μg/mL, 10 min at 37 °C, Sigma #L5266) and fixed with 4% paraformaldehyde in PBS. The cells were mounted to a slide using mounting medium containing DAPI and imaged using a confocal laser scanning microscope (Olympus FluoView® FV1000, Olympus, Center Valley, PA). Cellular uptake as a function of time was quantified by flow cytometry. DU145 cells were exposed to heat shock (43 °C/30 min incubation) or control (37 °C, continuous incubation). Eight hours post-heat shock, cells were incubated with 0.1 mg/mL of heat shock targeted or untargeted conjugates. At each time point, cells were washed, harvested, fixed in 1% formaldehyde in PBS, and analyzed by flow cytometry.

In vitro cytotoxicity of conjugates bearing the anticancer agent AHGDM

DU145 cells in 96 well plates (3×10^3 cells per well) were exposed to heat shock (43 °C/30 min incubation) or control (37 °C, continuous incubation). Eight hours post-heat shock, cells were incubated for four hours with increasing concentrations of heat shock targeted or untargeted conjugates or AHGDM free drug controls. After 72 h total incubation, cell viability was assessed using a 2-(2-methoxy-4-nitrophenyl)-3-(4-nitrophenyl)-5-(2,4-disulfophenyl)-2H-tetrazolium monosodium salt (WST-8) cell viability assay (Dojindo Molecular Technologies, Rockville, MD). IC_{50} values were calculated by non-linear regression and thermal enhancement defined as IC_{50} observed for control/IC_{50} observed following heat shock.

In vivo induction of heat shock via photothermal therapy

Anesthetized 6—12 week old athymic nu/nu mice were subcutaneously injected with 10^7 DU145 cells on each flank and tumors were allowed to grow until approximately 5—7 mm in diameter. Animals were then administered PEGylated gold nanorods (9.6 mg/kg) via tail vein injection. After 48 h, mice were anesthetized, and tumors were swabbed with 50% propylene glycol to enhance laser penetration depth [45]. Tumors on the right flank only were then radiated for 10 minutes using an 808 nm fiber coupled laser diode (Oclaro Inc., San Jose, CA) with collimating lens (Thorlabs, Newton, NJ). Intratumoral temperature was monitored using a 33 gauge needle thermocouple (Omega, Stamford, CT) and tumor temperature was maintained between 42 °C and 43 °C. Tumors on the left flank served as internal controls.

In vivo GRP78 expression in tumors following photothermal therapy

Eight hours following induction of heat shock, mice were euthanized and tumors on the right (laser) and left (control) flanks were removed and snap frozen in liquid nitrogen. Immunohistochemical analysis of GRP78 expression was then

Table 1 *Characteristics of HPMA copolymer conjugates.* Weight average molecular weight (M_w) and polydispersity (M_w/M_n) were estimated by size exclusion chromatography (SEC). The amount of the anticancer agent AHGDM present was quantified by UV spectrometry, and the amount of the GRP78 targeting peptide was quantified by amino acid analysis (HPLC method).

Polymer	Feed composition (mol%)					Polymer characteristics			
	HPMA	MA-GG-TT	MA-GFLG-AHGDM	MA-Tyr-$CONH_2$	APMA-FITC	Apparent M_w (kDa)	M_w/M_n	AHGDM content	WIFPWIQL content
HPMA-(GFLG-AH-GDM)	88	5	5	2	0	72.6	1.6	16.1 wt%	—
HPMA-(GFLG-AH-GDM)-WIFPWIQL	88	5	5	2	0	75.8	1.3	14.5 wt%	19.9 wt%
HPMA	93	5	0	2	0	83.9	1.6	—	—
HPMA-WIFPWIQL	93	5	0	2	0	72.4	1.6	—	20.9 wt%
HPMA-FITC	93	5	0	0	2	62.4	1.4	—	—
HPMA-FITC-WIFPWIQL	93	5	0	0	2	64.4	1.4	—	18.0 wt%

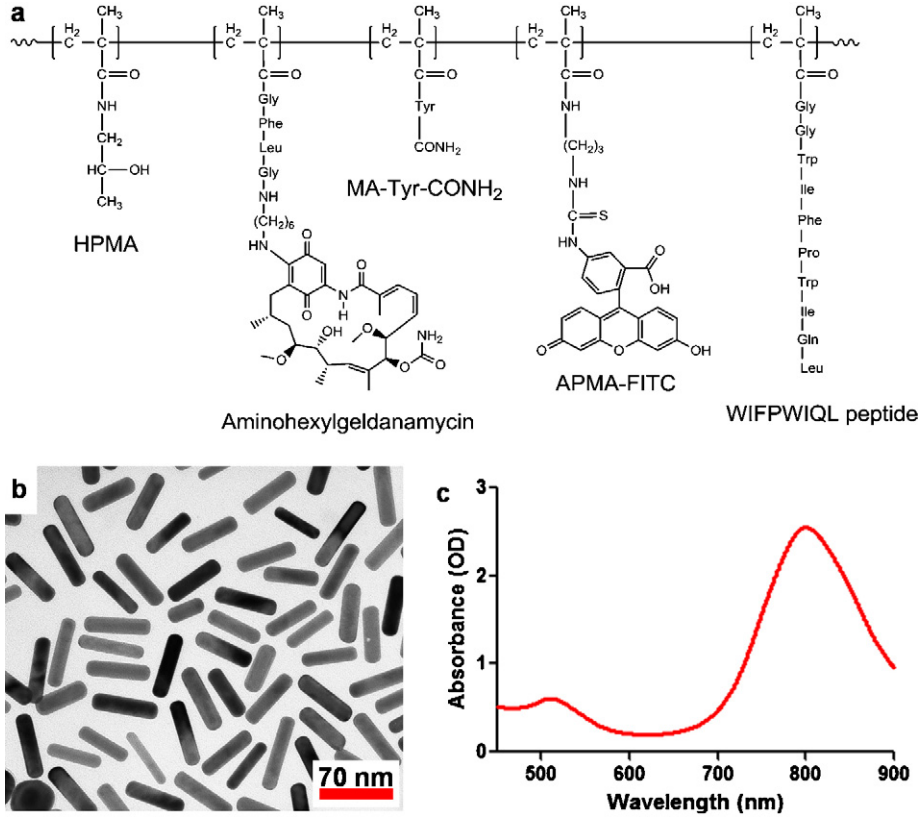

Figure 2 *HPMA copolymer schematic and gold nanorod characterization.* (a) Representative HPMA copolymer with all monomers used in the study listed. For individual polymer composition, see Table 1. (b) Transmission electron micrograph (TEM) and (c) light absorption profile of synthesized gold nanorods.

performed on 4-micron thick sections of formalin-fixed, paraffin-embedded tissues using a goat polyclonal anti-GRP78 antibody (Santa Cruz Biotechnology, Santa Cruz, CA) and a polyclonal rabbit anti-goat biotinylated antibody. Positive signal was visualized using a streptavidin-HRP system, utilizing DAB (3,3′-diaminobenzidine) as the chromogen. The sections were counterstained with hematoxylin. The sections were placed in iodine to remove any precipitates, and then dipped in sodium thiosulfate to clear the iodine. The sections were dehydrated in graded alcohols (70%, 95% 2× and 100% 2×), cleared in xylene, coverslipped and imaged.

Tumor accumulation and biodistribution

Prior to induction of heat shock via photothermal therapy, mice were intravenously administered via the tail vein a single bolus dose of 50 mg/kg ^{125}I radiolabeled conjugates (untargeted or heat shock targeted). At each time point, mice were euthanized, blood immediately collected, followed by blood perfusion with saline. Tumors and major organs were then collected and analyzed by gamma counting. Percent injected dose per gram of blood/tissue (%ID/g) was calculated and expressed as a function of time.

Results and discussion

To begin, the HPMA copolymers were synthesized via free radical polymerization and characterized (Fig. 2a, Table 1). Molecular weight for the conjugates varied from 60 to 80 kDa, and was maintained slightly above renal threshold to take advantage of the EPR effect. For drug containing conjugates, AHGDM content was approximately 15% by weight. To generate a targetable HPMA copolymer, the WIFPWIQL peptide was conjugated to the HPMA backbone via aminolysis of thiazolidine-2-thione side chains, resulting in copolymers with approximately 20% peptide content by weight. This peptide was chosen due to its known affinity to glucose-regulated protein-78 (GRP78), a member of the HSP70 family of proteins [46]. Previously, we have shown that this receptor—ligand approach can be used to effectively deliver HPMA copolymer-drug conjugates to prostate cancer cells [42]. Full details regarding the feed compositions and resulting polymer characteristics are given in Table 1.

Gold nanorods were used in this study because they have a greater light absorption cross section per unit size relative to those with other geometries (i.e. shells and spheres) [47], and are capable of inducing heat shock in tissue upon laser excitation [31,35,37—39,48]. Before use, the gold nanorods were grafted with a PEG surface coating to reduce the extent of protein adsorption and improve blood circulation time [49]. This resulted in a zeta potential of −10.0 mV. The aspect ratio (4.1), size (58.8 × 14.4 nm ± 6.5 × 2.1 nm) and therefore SPR peak at 800 nm was chosen as light at this wavelength is capable of penetrating tissue several centimeters (Fig. 2b and c). By this method, as determined

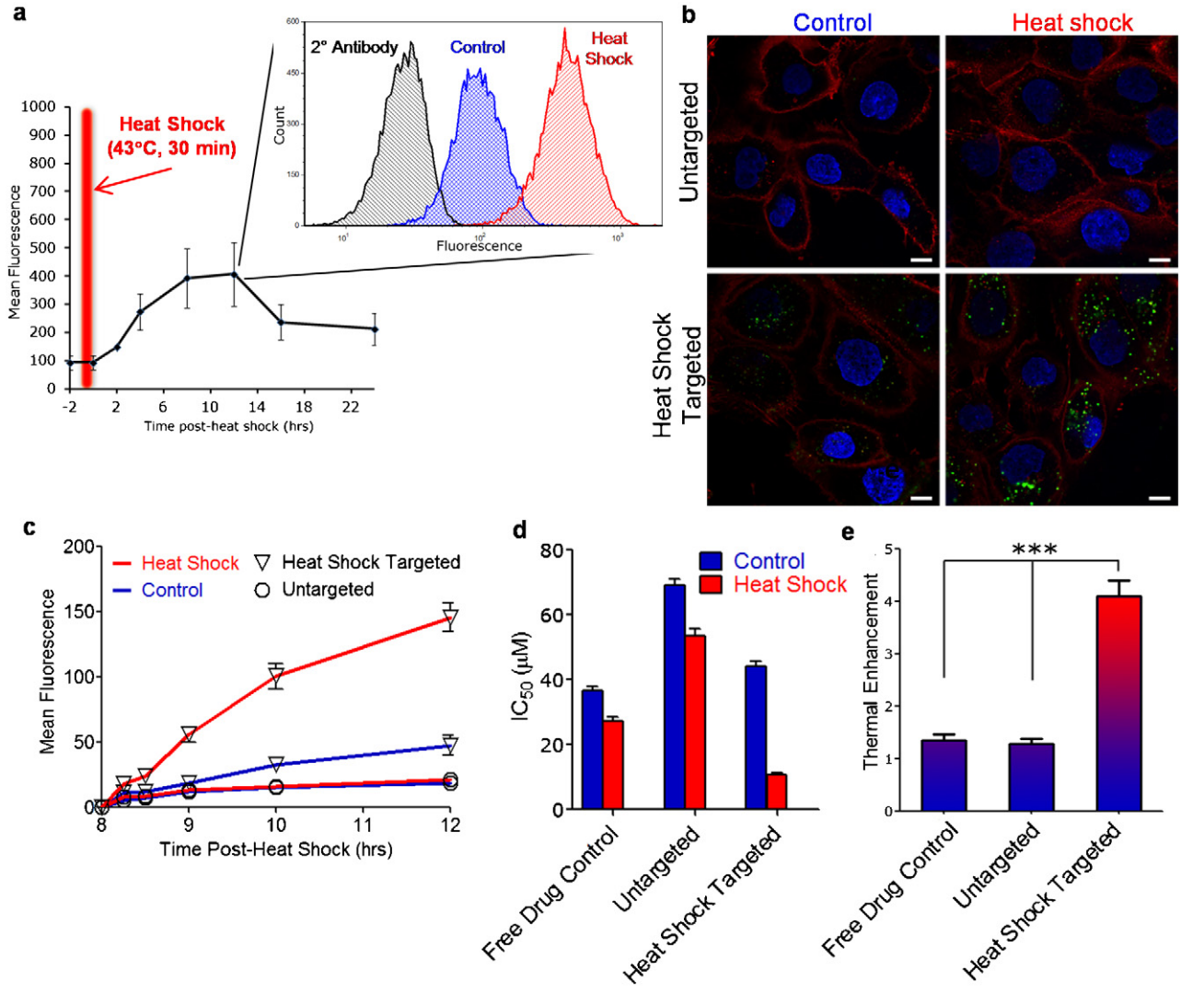

Figure 3 *In vitro investigation of heat shock targeting.* (a) After induction of heat shock, the cell surface expression of the heat shock protein GRP78 in prostate cancer cells is quantified with peak expression occurring at 12 h. (b,c) Cellular binding and uptake of fluorescently labeled (green) HPMA copolymers in cells. Scale bar, 10 μm. Prior treatment with heat shock results in significantly increased uptake of heat shock targeted conjugates. (d,e) Polymer-drug conjugate anti-cancer activity (IC_{50}) and related thermal enhancement of toxicity with prostate cancer cells. Treatment with heat shock causes increased toxicity to cells (lowered IC_{50}, greater thermal enhancement), particularly for those which are heat shock targeted. ***Indicates a statistically significant difference ($p < 0.001$) by one-way analysis of variance (ANOVA). Error bars represented as ±standard deviation.

in a previous study, 1.22% of the injected dose is delivered to the tumor [50].

To determine if heat shock could be used to regulate the targetability of these conjugates, the prostate cancer cell surface expression of GRP78 was measured as a function of time post-heat shock (43 °C, 30 min). This was done by incubation with an anti-GRP78 rabbit polyclonal antibody followed by evaluation of expression by flow cytometry. Indeed, it was observed that the receptor's expression increases after heat shock with maximum expression between 8 and 12 h post-heat shock (Fig. 3a).

Next, fluorescently labeled HPMA copolymers with and without the heat shock targeting peptide were introduced to cells eight hours post-heat shock (43 °C, 30 min) or control (37 °C, continuous incubation). Visualization by confocal microscopy (four hour incubation, Fig. 3b) and quantification by flow cytometry (selected time points, Fig. 3c) of uptake in cells indicates significantly increased binding and uptake of heat shock targeted conjugates which is in agreement with our previous results [42]. This observation was much more pronounced (three-fold increase), when the cells were first treated with heat shock due to increased receptor expression.

New conjugates containing the anticancer drug derivative AHGDM via a degradable linker were then prepared to determine if this increased uptake can be correlated with increased activity. Cells were heat shock treated as before, then exposed to the HPMA copolymer-AHGDM conjugates for four hours and evaluated for growth inhibition. In all groups (free drug, untargeted, and heat shock targeted),

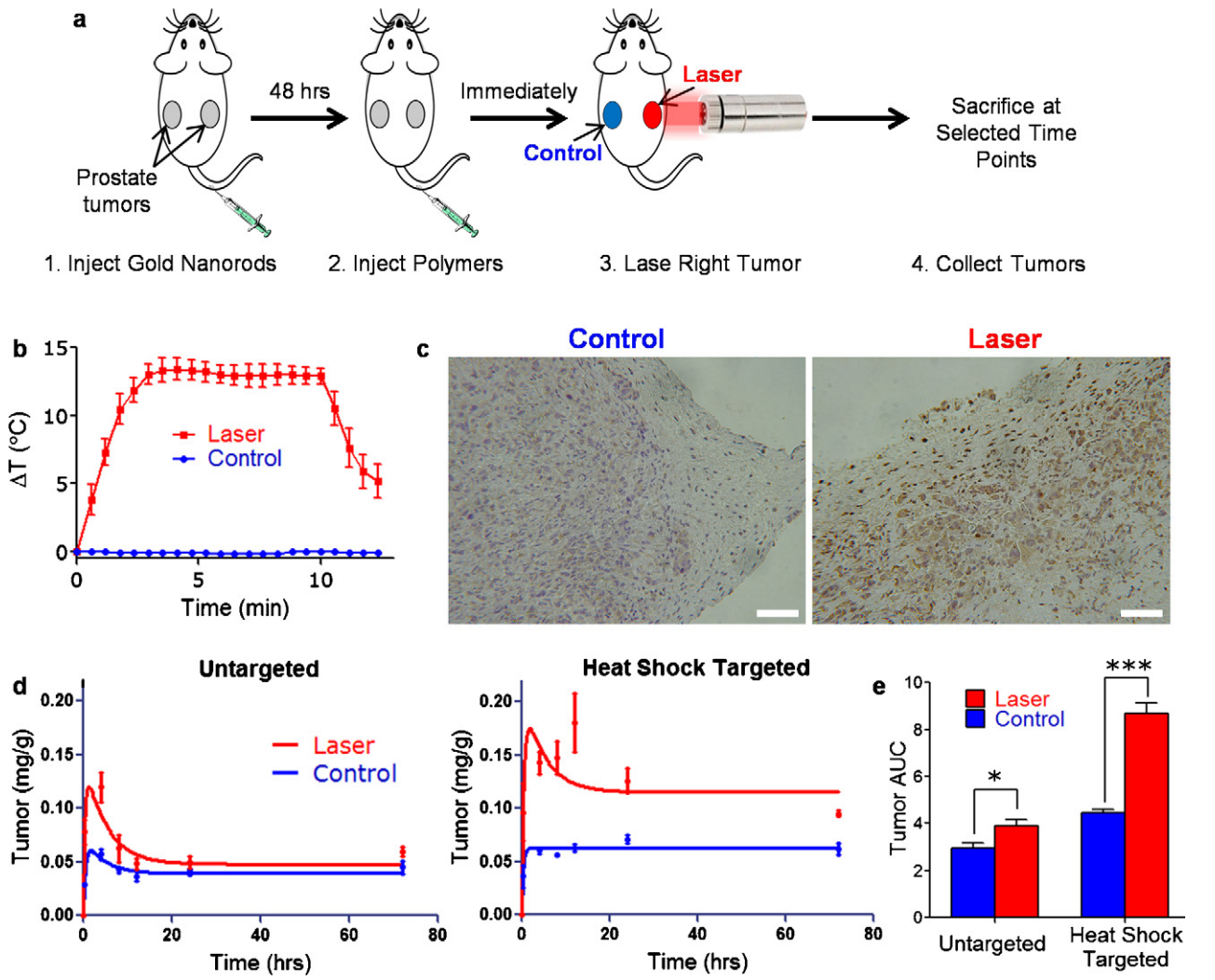

Figure 4 *Laser guided delivery of polymeric conjugates in mice*. (a) Schematic of experimental procedure. (b) Changes in intratumoral temperatures during laser radiation (10 min) of left (control) and right (laser) tumors. (c) Cell expression of heat shock protein GRP78 (red color) in prostate tumors with or without laser treatment. Scale bar, 50 μm. Tumors which have been laser radiated have higher expression of GRP78. (d) Tumor accumulation of radiolabeled polymers (untargeted and heat shock targeted) with or without laser treatment. Data expressed as experimental points with pharmacokinetic modeled lines. Laser radiation results in a burst accumulation (0—4 h), which is only maintained (>24 h) for the heat shock targeted polymers due to increased GRP78 expression. (e) Total area under the tumor concentration vs. time curve (AUC) indicates a four-fold increase in exposure to polymers. * and *** indicates a statistically significant difference ($p < 0.05$ and $p < 0.001$ respectively) by one-way analysis of variance (ANOVA). Error bars represented as ±standard deviation (b,e) and standard error of the mean (d).

treatment with heat shock resulted in greater activity (Fig. 3d). While this effect was only slight for free drug and untargeted conjugates, a four-fold thermal enhancement in conjugate activity was observed for those which were heat shock targeted (Fig. 3e).

Next, the overall hypothesis of enhancing the delivery of these conjugates to laser radiated tissue was tested in mice bearing prostate tumors. Mice bearing two tumors, one on each flank, were intravenously (i.v.) administered PEG coated gold nanorods and allowed 48 h for the particles to accumulate in the tumors via EPR (Fig. 4a) [50]. Radiolabeled conjugates (heat shock targeted and untargeted) were then administered i.v. followed immediately by laser radiation of the right tumor only for 10 minutes. During laser radiation the temperature in the right tumor was maintained between 42 °C and 43 °C by controlling laser power such that only moderate hyperthermia was induced to avoid vascular collapse at higher temperatures (Fig. 4b) [51]. It is important to note here that by directing the laser at the right tumor only, it is possible to directly compare the delivery of polymeric conjugates to tumors in the presence and absence of laser radiation in the same animal.

While the increased HSP expression profile of prostate cancer cells following heat shock was confirmed in vitro, it was necessary to confirm this phenomenon in vivo. The left (control) and right (laser treated) tumors were evaluated for GRP78 expression by immunohistochemistry. Heat shock treatment of the right tumors by laser resulted in increased HSP expression compared to the untreated tumors (Fig. 4c).

Following administration of the polymeric conjugates, a comparison of the laser radiated and control tumors 15 minutes and four hours following laser treatment indicates that a two-to-three fold increased burst accumulation occurred in the laser radiated tumors (Fig. 4d). This observation indicates that the treatment of tumors with heat causes increased tumor blood flow and augments the EPR effect by increasing vascular pore size [19,20,37]. This burst accumulation was not maintained after four hours for the untargeted conjugates. As intended in the treatment design, the heat shock targeted conjugates were retained in the radiated tumor up to 12 h after which elimination began to occur. This observation is supported by GRP78 expression data (Fig. 3a), which shows that HSP expression is reduced after 12 h. When this data is expressed as the total area under the tumor concentration vs. time curve (AUC), a four-fold increase in exposure is observed for tumors which have been laser radiated (Fig. 4e).

The biodistribution of the radiolabeled conjugates in major organs was also evaluated (see Supplementary data). Similar concentrations in the blood were observed over 72 h for untargeted and heat shock targeted conjugates. However, significant accumulation was observed for the heat shock targeted conjugate in the liver, spleen, and kidneys. We speculate that this non-specific accumulation is most likely due to the increased hydrophobic nature of the heat shock targeted conjugate due to the presence of the hydrophobic WIFPWIQL peptide (cLog $P = 3.9$). This increased hydrophobicity can potentiate interactions with biological tissues and increase uptake in reticuloendothelial system (RES) organs [52]. It is anticipated that such non-specific interactions can be minimized by reducing the hydrophobic nature of the conjugates by either reducing the targeting peptide content or utilizing more hydrophilic targeting moieties.

Polymer accumulation and elimination data was analyzed using a three compartment pharmacokinetic model linking the plasma and the tumor (see Supplementary data). The model was set up to differentiate between the tumor extracellular and intracellular space in order to understand the roles of laser treatment and targeting on the rate and extent of tumor accumulation and elimination. Laser treated tumors showed an increase in the rate of absorption into the tumor extracellular space whereas the rate of elimination was reduced for heat shock targeted conjugates, possibly due to improved intracellular delivery.

Conclusions

In summary, we have demonstrated that it is possible to direct the delivery of targeted polymer therapeutics using plasmonic photothermal therapy by exploiting the physiologic response of tumors to heat. These findings help overcome one of the limitations of polymer therapeutics which is poor tumor accumulation. By using laser directed application of heat via gold nanorods, a burst accumulation of the therapeutics in the region of interest is possible while they are at their highest concentration in the blood. By incorporation of a heat shock targeting ligand in the copolymer design, high concentration can be maintained as the targeting receptors become increasingly available following heat induction. Ultimately, in a clinical setting, we anticipate that clinicians will value this additional tool to help guide drug delivery to solid tumors.

Acknowledgements

The authors thank Dr. Khaled Greish for his help with the animal studies, Dr. Alexander Malugin for his help with the cell culture experiments and Sheryl Tripp at ARUP Laboratories for her help with the IHC staining. This research was supported by a Department of Defense Prostate Cancer Predoctoral Training Award (PC094496) as well as the National Institutes of Health (EB-R01EB7171) and the Utah Science, Technology, and Research (USTAR) Initiative.

Appendix A. Supplementary data

Supplementary data associated with this article can be found, in the online version, at http://dx.doi.org/10.1016/j.nantod.2012.04.002.

References

[1] D. Peer, J.M. Karp, S. Hong, O.C. Farokhzad, R. Margalit, R. Langer, Nature Nanotechnology 2 (2007) 751—760.
[2] M.J. Vicent, H. Ringsdorf, R. Duncan, Advanced Drug Delivery Reviews 61 (2009) 1117—1120.
[3] S.K. Hobbs, W.L. Monsky, F. Yuan, W.G. Roberts, L. Griffith, V.P. Torchilin, R.K. Jain, Proceedings of the National Academy of Sciences of the United States of America 95 (1998) 4607—4612.
[4] Y. Matsumura, H. Maeda, Cancer Research 46 (1986) 6387—6392.
[5] H. Maeda, J. Wu, T. Sawa, Y. Matsumura, K. Hori, Journal of Controlled Release 65 (2000) 271—284.
[6] T. Lammers, W. Hennink, G. Storm, British Journal of Cancer 99 (2008) 392—397.
[7] D.B. Pike, H. Ghandehari, Advanced Drug Delivery Reviews 62 (2009) 167—183.
[8] R. Duncan, Nature Reviews — Drug Discovery 2 (2003) 347—360.
[9] J. Kopecek, P. Kopecková, Advanced Drug Delivery Reviews 62 (2010) 122—149.
[10] R. Duncan, Nature Reviews — Cancer 6 (2006) 688—701.
[11] G. Oberdörster, E. Oberdörster, J. Oberdörster, Environmental Health Perspectives 113 (2005) 823—839.
[12] D.W. Grainger, Advanced Drug Delivery Reviews 61 (2009) 419.
[13] G. Oberdörster, Journal of Internal Medicine 267 (2010) 89—105.
[14] W.R. Sanhai, J.H. Sakamoto, R. Canady, M. Ferrari, Nature Nanotechnology 3 (2008) 242—244.
[15] L. Seymour, Y. Miyamoto, H. Maeda, M. Brereton, J. Strohalm, K. Ulbrich, R. Duncan, European Journal of Cancer 31 (1995) 766—770.
[16] R. Duncan, R. Gaspar, Molecular Pharmacology 8 (2011) 2101—2141.
[17] Q. Chen, A. Krol, A. Wright, D. Needham, M. Dewhirst, F. Yuan, International Journal of Hyperthermia 24 (2008) 475—482.
[18] M. Gnant, L. Noll, R. Terrill, P. Wu, A. Berger, H. Nguyen, T. Lans, B. Flynn, S. Libutti, D. Bartlett, Surgery 126 (1999) 890—899.
[19] G. Kong, R.D. Braun, M.W. Dewhirst, Cancer Research 60 (2000) 4440—4445.
[20] G. Kong, R.D. Braun, M.W. Dewhirst, Cancer Research 61 (2001) 3027—3032.

[21] A.T. Lefor, S. Makohon, N.B. Ackerman, Journal of Surgical Oncology 28 (1985) 297—300.
[22] M.L. Matteucci, G. Anyarambhatla, G. Rosner, C. Azuma, P.E. Fisher, M.W. Dewhirst, D. Needham, D.E. Thrall, Clinical Cancer Research 6 (2000) 3748—3755.
[23] K. Fujiwara, T. Watanabe, Pathology International 40 (2008) 79—84.
[24] B. Chen, M. Zhou, L. Xu, Journal of Thermal Biology 30 (2005) 111—117.
[25] L. Fajardo, A. Schreiber, N. Kelly, G. Hahn, Radiation Research 103 (1985) 276—285.
[26] B. Hildebrandt, P. Wust, O. Ahlers, A. Dieing, G. Sreenivasa, T. Kerner, R. Felix, H. Riess, Critical Reviews in Oncology/Hematology 43 (2002) 33—56.
[27] L. Xu, B. Chen, M. Zhou, Journal of Thermal Biology 31 (2006) 302—306.
[28] P. Wust, B. Hildebrandt, G. Sreenivasa, B. Rau, J. Gellermann, H. Riess, R. Felix, P.M. Schlag, Lancet Oncology 3 (2002) 487—497.
[29] S. Link, M.A. El-Sayed, International Reviews in Physical Chemistry 19 (2000) 409—453.
[30] X. Huang, P.K. Jain, I.H. El-Sayed, M.A. El-Sayed, Lasers in Medical Science 23 (2008) 217—228.
[31] E.B. Dickerson, E.C. Dreaden, X. Huang, I.H. El-Sayed, H. Chu, S. Pushpanketh, J.F. McDonald, M.A. El-Sayed, Cancer Letters 269 (2008) 57—66.
[32] L.R. Hirsch, R.J. Stafford, J.A. Bankson, S.R. Sershen, B. Rivera, R.E. Price, J.D. Hazle, N.J. Halas, J.L. West, Proceedings of the National Academy of Sciences of the United States of America 100 (2003) 13549—13554.
[33] D.P. O'Neal, L.R. Hirsch, N.J. Halas, J.D. Payne, J.L. West, Cancer Letters 209 (2004) 171—176.
[34] J.M. Stern, J. Stanfield, W. Kabbani, J.T. Hsieh, J.A. Cadeddu, Journal of Urology 179 (2008) 748—753.
[35] G. von Maltzahn, J.H. Park, A. Agrawal, N.K. Bandaru, S.K. Das, M.J. Sailor, S.N. Bhatia, Cancer Research 69 (2009) 3892—3900.
[36] P. Diagaradjane, A. Shetty, J.C. Wang, A.M. Elliott, J. Schwartz, S. Shentu, H.C. Park, A. Deorukhkar, R.J. Stafford, S.H. Cho, Nano Letters 8 (2008) 1492—1500.
[37] A.J. Gormley, K. Greish, A. Ray, R. Robinson, J.A. Gustafson, H. Ghandehari, International Journal of Pharmaceutics 415 (2011) 315—318.
[38] J.H. Park, G.v. Maltzahn, L.L. Ong, A. Centrone, T.A. Hatton, E. Ruoslahti, S.N. Bhatia, M.J. Sailor, Advanced Materials 22 (2010) 880—885.
[39] J.H. Park, G. von Maltzahn, M.J. Xu, V. Fogal, V.R. Kotamraju, E. Ruoslahti, S.N. Bhatia, M.J. Sailor, Proceedings of the National Academy of Sciences of the United States of America 107 (2010) 981—986.
[40] G. Von Maltzahn, J.H. Park, K.Y. Lin, N. Singh, C. Schwöppe, R. Mesters, W.E. Berdel, E. Ruoslahti, M.J. Sailor, S.N. Bhatia, Nature Materials 10 (2011) 545—552.
[41] B. Nikoobakht, M.A. El-Sayed, Chemistry of Materials 15 (2003) 1957—1962.
[42] N. Larson, A. Ray, A. Malugin, D.B. Pike, H. Ghandehari, Pharmaceutical Research 27 (2010) 2683—2693.
[43] V. Omelyanenko, P. Kopecková, C. Gentry, J. Kopecek, Journal of Controlled Release 53 (1998) 25—37.
[44] J.M. Walker, The Protein Protocols Handbook, 2nd ed., Humana Press Inc, Totowa, NJ, 1996.
[45] R.K. Wang, V.V. Tuchin, Journal of X-ray Science and Technology 10 (2002) 167—176.
[46] M.A. Arap, J. Lahdenranta, P.J. Mintz, A. Hajitou, Á. Sarkis, W. Arap, R. Pasqualini, Cancer Cell 6 (2004) 275—284.
[47] P.K. Jain, K.S. Lee, I.H. El-Sayed, M.A. El-Sayed, Journal of Physical Chemistry B 110 (2006) 7238—7248.
[48] X. Huang, I.H. El-Sayed, W. Qian, M.A. El-Sayed, Journal of the American Chemical Society 128 (2006) 2115—2120.
[49] T. Niidome, M. Yamagata, Y. Okamoto, Y. Akiyama, H. Takahashi, T. Kawano, Y. Katayama, Y. Niidome, Journal of Controlled Release 114 (2006) 343—347.
[50] A.J. Gormley, A. Malugin, A. Ray, R. Robinson, H. Ghandehari, Journal of Drug Targeting 19 (2011) 915—924.
[51] T.E. Dudar, R.K. Jain, Cancer Research 44 (1984) 605—612.
[52] D. Owens 3rd, N. Peppas, International Journal of Pharmaceutics 307 (2006) 93—102.

Adam Gormley received his B.S. degree in Mechanical Engineering from Lehigh University (Bethlehem, PA) in 2006 before entering the Bioengineering program at the University of Utah (Salt Lake City, UT). His dissertation work in Dr. Hamid Ghandehari's lab and interests lie in the field of nanotechnology, self-assembly, drug delivery and nanomedicine.

Nate Larson received his B.S. degree in Chemistry from the University of Utah (Salt Lake City, UT) in 2005. After spending several years in the pharmaceutical industry as a product development scientist, he entered the Pharmaceutics and Pharmaceutical Chemistry program at the University of Utah in 2008. His current dissertation work and interests are in nanomedicine, polymeric drug delivery, and pharmaceutical product development.

Shraddha S. Sadekar got her Bachelor's degree in Pharmaceutical Science from University of Mumbai. She joined the graduate program in the Department of Pharmaceutics and Pharmaceutical Chemistry at the University of Utah in 2007. Her research interests include polymeric drug delivery systems and pharmacokinetics of macromolecular systems.

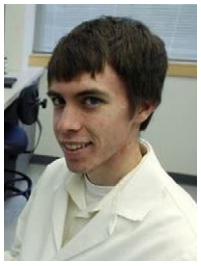

Ryan Robinson is a Biomedical Engineering senior undergraduate at the University of Utah who graduated from Taylorsville High (Taylorsville, UT) as valedictorian in 2009, simultaneously receiving his Associate of Science degree from SLCC. Ryan then began nanoscience research in Dr. Hamid Ghandehari's lab to pursue his interest in nanotechnology, and he continues to do research there today. Ryan plans to graduate from the University of Utah in the fall of 2012, at which point he plans to begin a PhD in Biomedical Engineering.

Dr. Abhijit Ray has a PhD in Organic Chemistry and has worked on fluoroquinolones and oxazolidinones in the new drug discovery research division of Ranbaxy Laboratories Limited. He is currently a Research Assistant Professor in the Department of Pharmaceutics and Pharmaceutical Chemistry at the University of Utah, with research interests in macromolecular delivery of chemotherapeutic agents to solid tumors. His current research involves the synthesis of polymeric macromolecules and inorganic nanoparticles (gold/silica) for targeted delivery with theranostic applications.

Dr. Hamid Ghandehari is Professor at the Departments of Pharmaceutics & Pharmaceutical Chemistry and Bioengineering, Director of Center for Nanomedicine and Co-Director of the Nano Institute of Utah, University of Utah. His research focuses on design of new polymers for gene therapy, targeted delivery of polymer therapeutics, and assessing the biocompatibility of nanoconstructs. Dr. Ghandehari is Chief Editor of Advanced Drug Delivery Reviews, Fellow of the American Institute for Medical and Biological Engineering and the American Association of Pharmaceutical Scientists. He received his BS in Pharmacy (1989) and PhD in Pharmaceutics and Pharmaceutical Chemistry (1996) from the University of Utah.